Ligand Binding Sites in *Escherichia coli* Inorganic Pyrophosphatase: Effects of Active Site Mutations†

Teppo Hyytiä,‡,§ Pasi Halonen,‡,§ Anu Salminen,|| Adrian Goldman,⊥ Reijo Lahti,*,|| and Barry S. Cooperman*,‡

Department of Chemistry, University of Pennsylvania, Philadelphia, Pennsylvania 19104-6323, Department of Biochemistry, University of Turku, FIN-20500, Turku, Finland, and Institute of Biotechnology, University of Helsinki, P.O. Box 56, FIN-00014, Helsinki, Finland

Received January 8, 2001; Revised Manuscript Received February 15, 2001

ABSTRACT: Type I soluble inorganic pyrophosphatases (PPases) are well characterized both structurally and mechanistically. Earlier we measured the effects of active site substitutions on pH−rate profiles for the type I PPases from both *Escherichia coli* (E-PPase) and *Saccharomyces cerevisae* (Y-PPase). Here we extend these studies by measuring the effects of such substitutions on the more discrete steps of ligand binding to E-PPase, including (a) Mg^{2+} and Mn^{2+} binding in the absence of added ligand; (b) Mg^{2+} binding in the presence of either P_i or hydroxymethylbisphosphonate (HMBP), a competitive inhibitor of E-PPase; and (c) P_i binding in the presence of Mn^{2+}. The active site of a type I PPase has well-defined subsites for the binding of four divalent metal ions (M1−M4) and two phosphates (P1, P2). Our results, considered in light of pertinent results from crystallographic studies on both E-PPase and Y-PPase and parallel functional studies on Y-PPase, allow us to conclude the following: (a) residues E20, D65, D70, and K142 play key roles in the functional organization of the active site; (b) the major structural differences between the product and substrate complexes of E-PPase are concentrated in the lower half of the active site; (c) the M1 subsite is functionally isolated from the rest of the active site; and (d) the M4 subsite is an especially unconstrained part of the active site.

Soluble inorganic pyrophosphatase (EC 3.6.1.1; PPase),[1] which hydrolyzes inorganic pyrophoshate (PP_i) to inorganic phosphate (P_i), is an essential enzyme (*1*−*3*), providing a thermodynamic pull for many biosynthetic reactions (*4*). Two types of soluble PPases are known (*5*−*7*). Structural and functional properties of type I PPases have been analyzed quite extensively, with the best studied being those from *Escherichia coli* (E-PPase) and the cytosol of *Saccharomyces cerevisiae* (Y-PPase). A simplified kinetic model for the catalysis of type I PPases at fixed pH (7.2) is shown in Scheme 1 (*8*−*12*). Noteworthy in this scheme is the binding of two Mg^{2+} ions in the absence of substrate and of two additional Mg^{2+} ions in the presence of substrate.

E-PPase is a homohexamer and Y-PPase is a homodimer with subunit molecular masses of 20 kDa (*13*) and 32 kDa (*14*), respectively. We have recently identified 13 polar residues at the active site as being important for enzyme activity through a combination of sequence comparisons (*5*, *15*), measurements of the enzymatic activity of active site variants (*16*−*20*), and X-ray crystallography (*21*, *22*). Results discussed in these publications have clearly demonstrated a remarkable conservation of the type I PPase active site throughout evolution, and have permitted formulation of a detailed mechanism for PPase catalysis.

Scheme 1 implies the existence of six defined ligand subsites at the enzyme active site, four for the binding of the metal ions (subsites M1, M2, M3, and M4) and two for the binding of the two product P_is (P1 and P2). PP_i binding has been recently shown to overlap sites P1 and P2 (*22*). Crystallographic studies of E-PPase have thus far located only three of the six putative subsites—sites M1 and M2 for Mg^{2+} binding in the absence of a phosphoryl ligand such as P_i or a PP_i analogue (*23*, *24*), and site P1, seen with bound sulfate in the absence of divalent metal ion (*25*). More significant results have been obtained for Y-PPase, for which high-resolution structures are now available for the Mn_2E, $Mn_2E(MnP_i)_2$, and $Mn_2EFMn_2PP_i$ complexes (*21*, *22*, *26*). The latter two structures, in particular, confirm the existence of the six ligand sites. In addition to the ligand subsites at the active site, a seventh ligand subsite, with a stoichiometry of one per two subunits (*27*), has been detected at the trimer−trimer interface of E-PPase (*23*, *24*).

Earlier we determined the effect of active site substitutions on pH−rate profiles for both E-PPase (*16*) and Y-PPase (*20*). Here we explore the effects of such substitutions on the more discrete steps of ligand binding to E-PPase, specifically, on (a) Mg^{2+} and Mn^{2+} binding to E-PPase in the absence of

† This work was supported by grants from the NIH (DK13212) and the Academy of Finland (47513).

* To whom correspondence should be addressed. B.S.C.: tel 215-898-6330, fax 215-898-2037, email cooprman@pobox.upenn.edu. R.L.: tel 358-2-333 6845, fax 358-2-333 6845, email reijo.lahti@utufi.

‡ University of Pennsylvania.

§ Current address: Department of Biochemistry, University of Turku, FIN-20500, Turku, Finland.

|| University of Turku.

⊥ University of Helsinki.

[1] Abbreviations: E-PPase, *Escherichia coli* inorganic pyrophosphatase; EGTA, ethylene glycol bis(β-aminoethyl ether)-*N*,*N*,*N*′,*N*′-tetraacetic acid; HMBP, hydroxymethylbisphosphonate; PPase, inorganic pyrophosphatase; PP_i, inorganic pyrophosphate; P_i, inorganic phosphate; Y-PPase, *Saccharomyces cerevisiae* inorganic pyrophosphatase; WT, wild-type.

10.1021/bi010049x CCC: $20.00
Published on Web 03/22/2001

Scheme 1: Minimal Scheme of Type I-PPase Catalysis[a]

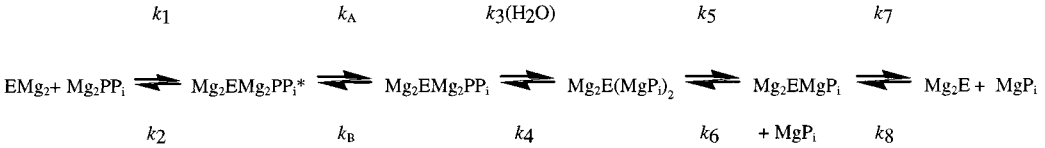

[a] The sequence of catalytic events in the active site includes substrate binding to preformed enzyme complex containing two Mg^{2+} ions/subunit, isomerization of the resulting complex, P−O bond breakdown by direct attack of water, and stepwise dissociation of two phosphate molecules.

added ligand; (b) Mg^{2+} binding to E-PPase in the presence of either P_i or hydroxymethylbisphosphonate (HMBP), a competitive inhibitor of E-PPase; and (c) P_i binding in the presence of Mn^{2+}. We focus on the 13 polar active site residues involved in interactions with subsites M1−M4, P1, and P2, either directly or via an intervening water. These residues include 5 Asp, 2 Glu, 3 Lys, 1 Arg, and 2 Tyr. We employ variants either conserving charge (D/E, E/D, K/R, R/K) or conserving shape (Y/F). For a charged residue, the effects of the substitution indicate the sensitivity of ligand binding to the precise placement of the charge in question, whereas Y/F substitution examines the dependence of ligand binding on the presence of the Tyr hydroxyl. Comparison of our results with the recently determined crystal structures referred to above allows evaluation of the steric and electrostatic requirements of interactions identified in these structures.

EXPERIMENTAL PROCEDURES

Materials. Wild-type E-PPase (*28*) and E-PPase variants free of contamination with wild-type enzyme (*16*) were prepared and purified as described. The disodium salt of HMBP was obtained as a gift from F. H. Ebetino (Procter and Gamble Pharmaceuticals).

Methods. All experiments were performed at pH 7.2 at an ionic strength of 0.1 M. Enzyme concentrations are expressed as monomer. Protein concentrations were determined by Bradford assay (Pierce). Initial rates of PP_i hydrolysis at 25 °C (*29*) and equilibrium dialysis experiments at 23 ± 2 °C (*30*) were performed as described. The following buffers were employed: (a) Mg^{2+} binding—Tris-HCl buffer (0.1 M) containing 20−50 μM EGTA; (b) Mg^{2+} binding in the presence of P_i—Tris-HCl buffer (0.04 M) containing 50 μM EGTA, 20 mM KH_2PO_4; (c) Mg^{2+} binding in the presence of 100 μM HMBP—as in (a); (d) Mn^{2+} binding—Tris-HCl buffer (0.1 M); (e) P_i binding in the presence of Mn^{2+}—0.083 M TES, 0.017 M KCl, 0.1 mM $MnCl_2$. Mg^{2+} and Mn^{2+} concentrations were determined by atomic absorption spectrometry at 285.2 and 279.5 nm, respectively. P_i determinations were carried out by an automatic P_i analyzer (*29*). Enzyme-containing samples used for P_i determination were deproteinized by pretreatment with 0.2 M perchloric acid, followed by centrifugation and dilution of supernatant to an appropriate concentration.

CALCULATIONS

Fitting of equations used in this work was performed using a program for nonlinear regression analysis (*31*, version 3.55) and MicroMath Scientist (version 2.01, MicroMath, Inc). Plots were constructed with SigmaPlot (version 2.01, Jandel).

Mg^{2+} or Mn^{2+} Binding. Values of dissociation constants for Mg^{2+} or Mn^{2+} binding of up to 2.5 equiv per E-PPase monomer were obtained by fitting equilibrium dialysis binding data to eq 1 (see ref *27*), which is derived assuming that M^{2+} binding to the interface occurs independently of M^{2+} binding to the active site, and that all six monomers are identical. Here, n is the number of divalent metal ions bound per E-PPase monomer, as determined by equilibrium dialysis, K_1 and K_2 are the macroscopic dissociation constants for M^{2+} binding to the active site, and K_{in} is the dissociation constant for binding to each of the three identical interface sites per hexamer, i.e., one per dimer. These constants are designated K_{g1}, K_{g2}, and $K_{g:in}$ and K_{n1}, K_{n2}, and $K_{n:in}$ for Mg^{2+} and Mn^{2+}, respectively. In the equations below, E is expressed as monomer concentration and D is expressed as dimer concentration.

$$n/\text{monomer} = 0.5 \times \{[M^{2+}]/([M^{2+}] + K_{in})\} + (K_2[M^{2+}] + 2[M^{2+}]^2)/(K_1K_2 + K_2[M^{2+}] + [M^{2+}]^2) \quad (1)$$

where $K_1 = [E][M^{2+}]/[EM^{2+}]$, $K_2 = [EM^{2+}][M^{2+}]/[EM_2]$, $K_{in} = [M][D]_t/[MD]_t$; and $[D]_T = [D]_t + [MD]_t$, $[D]_t = [D] + [DM] + [DM_2] + [DM_3] + [DM_4]$, $[MD]_t = [MD] + [MDM] + [MDM_2] + [MDM_3] + [MDM_4]$.

Mg^{2+} Binding in the Presence of Phosphoryl Ligands. We assume that Mg^{2+} binds to up to 4.5 sites within the E-PPase monomer in the presence of either P_i or HMBP, 4 per active site as seen in the Y-PPase complex $Mn_2E(MnP_i)_2$ plus 0.5 at the interface. Values of apparent dissociation constants for Mg^{2+} binding to these sites were obtained by fitting equilibrium dialysis binding data to eq 2, which was derived on the basis of the following considerations: (a) $[Mg^{2+}]_t$ refers to all forms of Mg^{2+} not bound to enzyme; i.e., it includes all Mg_xL terms where L is P_i or HMBP and x is equal to 1 or 2; (b) K'_{g1}, K'_{g2}, K_{g3}, and K_{g4} are the macroscopic dissociation constants for the binding of the first, second, third, and fourth metal ions to the active site in the presence of phosphoryl ligand, respectively; (c) for simplicity, we may assume that $K_{g3} = K_{g4} = K_{g3/4}$, as both WT and variant PPase fits to the Mg^{2+} binding data in the presence of either 20 mM P_i or 100 μM HMBP were not improved significantly when K_{g3} was allowed to be different from K_{g4}; and (d) $K_{g:in}$ is assumed to have the same value as in the absence of phosphoryl ligands, since these ligands do not interact with the interface site.

$$n/\text{monomer} = 0.5 \times \{[M^{2+}]_t/([M^{2+}]_t + K_{in})\} + \text{Num/Den} \quad (2)$$

where $\text{Num} = K'_{g2}K_{g3/4}^2[M^{2+}] + 2K_{g3/4}^2[M^{2+}]^2 + 3K_{g3/4}[M^{2+}]^3 + 4[M^{2+}]^4$ and $\text{Den} = K'_{g1}K'_{g2}K_{g3/4}^2 + K'_{g2}K_{g3/4}^2[M^{2+}] + K_{g3/4}^2[M^{2+}]^2 + K_{g3/4}[M^{2+}]^3 + [M^{2+}]^4$. In the presence of P_i, K'_{g1} is designated K^p_{g1}, K'_{g2} is designated K^p_{g2}, and $K'_{g3/4}$ is designated $K^p_{g3/4}$. In the presence of HMBP, K'_{g1} is designated K^{pp}_{g1}, K'_{g2} is designated K^{pp}_{g2}, and $K'_{g3/4}$ is designated $K^{pp}_{g3/4}$.

Table 1: Mg^{2+} and Mn^{2+} Binding[a]

E-PPase	K_{g1} (mM)	K_{g2} (mM)	$K_{g:in}$ (mM)	K_{n1} (μM)	K_{n2} (mM)	$K_{n:in}$ (mM)
WT	0.076 ± 0.002	6.6 ± 0.6	2.0	6 ± 1	0.34 ± 0.04	0.35
WT + 0.5 mM Mg^{2+} [b]				21 ± 4	0.40 ± 0.05	0.40
WT + 5.0 mM Mg^{2+} [b]				135 ± 8	1.4 ± 0.1	0.45
E20D	0.132 ± 0.009	>50	8.0	–	–	–
K29R	0.072 ± 0.002	3.3 ± 0.2	3.0	9 ± 3	0.21 ± 0.05	0.20
E31D	0.067 ± 0.002	2.3 ± 0.2	2.5	–	–	–
R43K	0.085 ± 0.004	4.0 ± 0.5	3.5	7 ± 3	0.19 ± 0.05	0.20
Y55F	0.068 ± 0.003	2.7 ± 0.4	2.5	–	–	–
D65E	0.51 ± 0.02	7 ± 1	6.5	94 ± 13	0.46 ± 0.06	0.30
D67E	0.152 ± 0.006	13 ± 4	1.5	11 ± 1	0.69 ± 0.07	0.20
D70E	0.088 ± 0.002	4.1 ± 0.3	2.5	7 ± 1	0.46 ± 0.04	0.45
D97E	0.073 ± 0.002	3.4 ± 0.3	3.5	–	–	–
D102E	0.219 ± 0.005	3.6 ± 0.3	3.0	9 ± 3	0.26 ± 0.07	0.25
K104R	0.094 ± 0.003	3.6 ± 0.3	3.5	–	–	–
Y141F	0.087 ± 0.004	4.4 ± 0.5	2.0	10 ± 4	0.16 ± 0.05	0.15
K142R	0.118 ± 0.004	16 ± 5	1.0	9 ± 2	0.21 ± 0.04	0.20
D97V	0.133 ± 0.005	8 ± 2	1.0	–	–	–
D102V	0.87 ± 0.03	27 ± 13	1.5	–	–	–
D26S	0.085 ± 0.007	10 ± 5	–[c]	–	–	–
K34R	0.080 ± 0.003	11 ± 2	2.0	–	–	–
E98V	0.084 ± 0.007	6 ± 1	4.0	–	–	–
H136Q	0.057 ± 0.005	2.8 ± 0.6	2.5	–	–	–
H140Q	0.122 ± 0.004	8 ± 2	1.0	–	–	–

[a] Enzyme concentration: Mg^{2+} binding, 0.3−1.0 mM; Mn^{2+} binding, 0.3 mM. Data for Mg^{2+} binding to WT-PPase (*10*) and the variants E20D (*18*), Y55F & K104R (*19*), D97E (*30*), and H136Q & H140Q (*32*) were obtained previously, and refit to eq 1, taking the interface site into account. For WT-E-PPase, considerably lower values of K_{g1} and K_{in} (although not K_{g2}) were recently found in non-Tris-containing buffers (*33*) due to a Tris interaction with enzyme. However, this interaction should not greatly affect the conclusions drawn in this work, which only concern differences in ligand affinity between variants and wild-type. [b] Mn^{2+} binding only. [c] Assumed to be infinite (*27*).

P_i Binding. Values of dissociation constants for P_i binding to the high-affinity site on E-PPase were fit to binding data using eq 3, where n is equal to the stoichiometry of bound P_i per E-PPase subunit, K_p is the apparent dissociation constant describing this binding, and $[P_i]_t$ refers to all forms of P_i not bound to enzyme; i.e., P_i plus MnP_i.

$$n = [P_i]_t/(K_p + [P_i]_t) \quad (3)$$

Initial Rates of PP_i Hydrolysis. Values of $1/v_i$ in the presence of HMBP were fit to eq 4 describing competitive inhibition.

$$1/v_i = 1/V_{max} + K_m(1 + [HMBP]/K_i)/[MgPP_i]V_{max} \quad (4)$$

RESULTS

$Mg^{2+}$and Mn^{2+} Binding. The three distinct sites of divalent metal ion binding to E-PPase in the absence of substrate, M1 and M2 at the active site and M_{in} at the trimer−trimer interface, bind with stoichiometries per subunit of 1.0, 1.0, and 0.5, respectively (*23, 24*). To determine the effects of mutation on such binding, equilibrium dialysis measurements were carried out in the absence of substrate at pH 7.2 on WT-PPase and 20 variants. Sample data for variants in which substitutions are made in residues directly binding to M1 are shown in Figure 1. The results obtained were fit to eq 1, giving the dissociation constants summarized in Table 1.

The fitting procedure required setting initial values for each of the three constants K_{g1}, K_{g2}, and $K_{g:in}$ and initially yielded an ambiguous result. In most cases, $K_{g2} > K_{g1}$, $K_{g:in}$ regardless of initial values. However, when initial K_{g1} < initial $K_{g:in}$, the fitted K_{g1} < fitted $K_{g:in}$, and when initial K_{g1} > initial $K_{g:in}$, the fitted K_{g1} > fitted $K_{g:in}$. For example, for WT-PPase

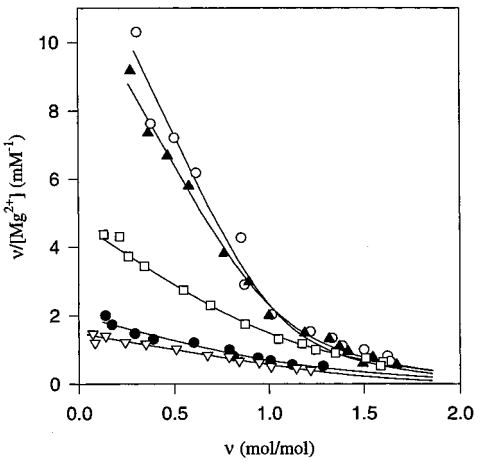

FIGURE 1: Scatchard plots of Mg^{2+} binding to WT-E-PPase and several E-PPase variants. Lines are fit to eq 1, using parameter values found in Table 1. Wild-type (O), D65E (●), D70E (▲), D102E (□), D102V (▽).

we obtained two sets of fitted values [K_{g1}, K_{g2}, $K_{g:in}$: 0.076, 6.6, 2.0 (Table 1) and 0.38, 18, 0.035, all values in millimolar], each of which fit our data quite well. This ambiguity was resolved by measuring Mg^{2+} binding to the D26S variant which lacks the interface site [Asp 26 residues from two subunits form part of the interface binding site; (*23, 24, 27*)]. The D26S variant shows reduced binding stoichiometry, as expected, and has K_{g1} and K_{g2} values of 0.085 ± 0.007 and 10 ± 5 mM, respectively. The K_{g1} value for D26S clearly shows that for WT-PPase, K_{g1} < $K_{g:in}$, since it is essentially identical to the value for WT-PPase obtained when initial K_{g1} < initial $K_{g:in}$, but is 4 times lower than the value obtained when initial K_{g1} > initial $K_{g:in}$. Thus, the

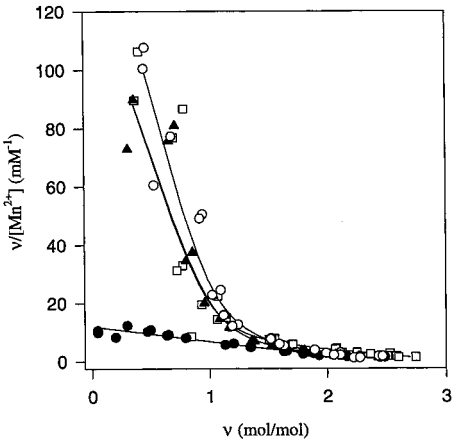

FIGURE 2: Scatchard plots of Mn^{2+} binding to WT-E-PPase and several E-PPase variants. Lines are fit to eq 1, using parameter values found in Table 1. Wild-type (○), D65E (●), D70E (▲), D102E (□).

values in Table 1 were obtained setting initial K_{g1} < initial $K_{g:in}$.

Earlier we had interpreted equilibrium dialysis studies of Mg^{2+} binding to WT-PPase and to several active site variants (*18*, *19*, *30*, *32*) as reflecting binding to sites M1 and M2 only. Reinterpretation of these data according to eq 1, which takes the interface site into account, has little effect on K_{g1}, but significantly increases K_{g2}. The resulting large difference in magnitudes of K_{g1} and K_{g2}, not only for WT-PPase but also for virtually all the variants studied, has as a consequence that these macroscopic constants closely approximate microscopic dissociation constants for ordered binding to specific sites in PPase: K_{g1} to M1 and K_{g2} to M2 (see Discussion).

Besides D26S, the other 19 variants to which Mg^{2+} binding was measured include conservative (D/E, R/K, Y/F) substitutions at each of 13 conserved active site polar residues as well as 2 nonconservative variants within this group, D97V and D102V. The additional four variants include two strongly conserved polar residues not involved functionally at the active site, K34R and E98V, and two (H136Q and H140Q) at the trimer−trimer interface (*32*). Only variants at positions 65 and 102 show a sizable increase in K_{g1}; the D65E and D102E substitutions lead to 7- and 3-fold increases, respectively, whereas D102V substitution leads to an 11-fold increase. By contrast, all other substitutions, including D97V and E98V, have little effect on K_{g1}.

As K_{g2} describes binding to a weak site, substitutions leading to a further weakening are difficult to measure accurately. However, E20D and D102V substitution clearly cause large decreases in affinity (> 8-fold and ∼4-fold, respectively), whereas most other substitutions have smaller effects, with several (e.g., E31D, Y55F, and H136Q) actually increasing affinity. Finally, whereas the great majority of substitutions have only small effects on $K_{g:in}$, two (E20D and D65E) lead to significant increases (3−4-fold), demonstrating that some effects of active site substitution can be propagated to the interface.

Mn^{2+} binding to WT-PPase and eight conservative active site variants was carried out and analyzed in an exactly analogous fashion to Mg^{2+} binding, except that a lower enzyme concentration was used because the affinities for Mn^{2+} are higher. Fitting the binding data to eq 1 yields the values for K_{n1}, K_{n2}, and $K_{n:in}$ shown in Table 1. Shown in Figure 2 are sample data for variants at the same positions as those shown in Figure 1. Each of the sites is apparently competed for by Mg^{2+} as shown by the increase in all three apparent dissociation constants for WT-PPase as a function of added Mg^{2+}. Paralleling the results with Mg^{2+}, most of the variants tested showed only minor effects on K_{n1}, K_{n2}, and $K_{n:in}$, and D65E substitution gave a large (14-fold) increase in K_{n1}. Three notable differences between Mn^{2+} and Mg^{2+} binding are that D102E substitution has little effect on K_{n1}, D65E substitution has little effect on $K_{n:in}$, and R43K substitution results in a 1.8-fold decrease in K_{n2}.

Mg^{2+} Binding in the Presence of P_i. Measured at pH 7.2, added P_i (20 mM) raises the stoichiometry of Mg^{2+} bound to WT-PPase (Figure 3), corresponding to the formation of the $Mg_2E(MgP_i)_2$ complex, in equilibrium with Mg_2EMg_2-PP_i (Scheme 1). The data obtained for WT- and variant PPases were fit to eq 2, as described under Calculations, giving the parameter values shown in Table 2. Comparing Tables 1 and 2, it is clear that for all of the PPases tested

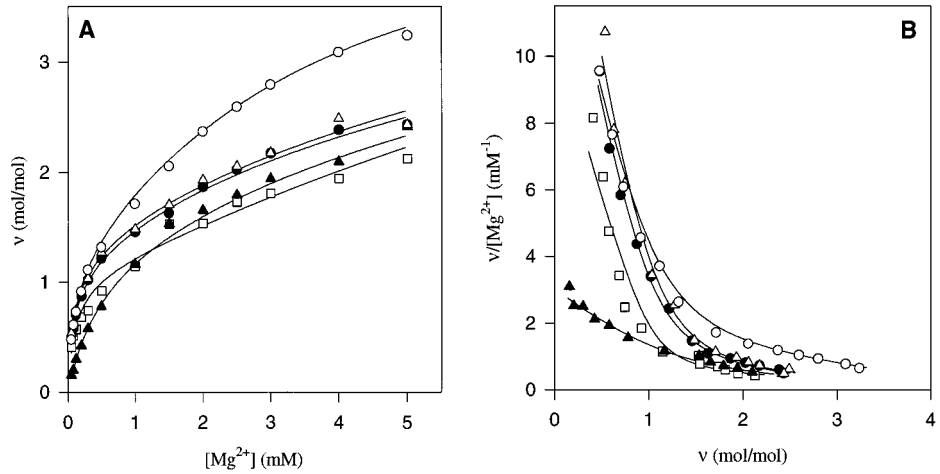

FIGURE 3: Mg^{2+} binding to WT-E-PPase and several E-PPase variants in the presence of 20 mM P_i. Lines are fit to eq 2, using parameter values found in Table 2. Wild-type (○), E20D (□), K29R (●), D65E (▲), K142R (△). (A) Binding curves. (B) Scatchard plots. Data are shown for variants having weaker Mg^{2+} binding than wild-type, i.e., increased R^p_{ov}, (see Table 2).

Table 2: Mg^{2+} Binding in the Presence of 20 mM P_i[a]

E-PPase	K^p_{g1} (mM)	K^p_{g2} (mM)	$K^p_{g3/4}$ (mM)	R^p_{ov}
WT	0.069 ± 0.003	1.1 ± 0.1	4.3 ± 0.3	1.00 ± 0.13
E20D	0.093 ± 0.007	4.5 ± 1.2	10 ± 3	20 ± 10
K29R	0.066 ± 0.003	1.9 ± 0.2	12 ± 1.5	12 ± 2
E31D	0.068 ± 0.002	1.9 ± 0.2	10 ± 1	9 ± 2
R43K	0.064 ± 0.002	1.7 ± 0.2	7.9 ± 0.6	5 ± 1
Y55F	0.056 ± 0.002	1.2 ± 0.1	10 ± 1	5 ± 1
D65E	0.34 ± 0.01	2.3 ± 0.3	12 ± 2	14 ± 4
D67E	0.082 ± 0.004	1.4 ± 0.2	4.8 ± 0.4	1.3 ± 0.2
D70E	0.073 ± 0.003	1.9 ± 0.2	12 ± 2	12 ± 3
D97E	0.061 ± 0.003	1.3 ± 0.2	4.2 ± 0.3	1.1 ± 0.2
D102E	0.20 ± 0.01	0.66 ± 0.07	5.9 ± 0.5	1.2 ± 0.2
K104R	0.065 ± 0.004	1.5 ± 0.2	6.2 ± 0.6	2.7 ± 0.5
Y141F	0.051 ± 0.003	2.8 ± 0.1	2.8 ± 0.1	1.0 ± 0.1
K142R	0.058 ± 0.003	2.7 ± 0.3	11 ± 1.5	15 ± 3
D97V	0.096 ± 0.006	1.5 ± 0.3	25 ± 12	43 ± 30

[a] Enzyme concentration 0.8−1.0 mM.

K^p_{g1} is approximately equal to K_{g1}, so that added P_i has little effect on binding to site M1.

Adding P_i increases the affinity of the second Mg^{2+} bound to the active site (i.e., $K_{g2} > K^p_{g2}$), with the effect on WT-PPase being 6-fold, and the effects on the variants varying from 1.2-fold (E31D) to >11-fold (E20D). As with K_{g2}, most substitutions have only a modest effect on K^p_{g2}, and, again, the largest reduction in affinity (4-fold) results from E20D substitution. These similarities suggest that, for WT-PPase and some variants, K^p_{g2}, like K_{g2}, provides an approximate measure of dissociation from site M2. However, for other variants K^p_{g2} is not much less than $K^p_{g3/4}$, so that the second, third, and fourth Mg^{2+} bound per monomer (exclusive of the interface) would be expected to distribute among sites M2, M3, and M4, eliminating any clear linkage between the macroscopic constants and constants reflecting dissociation from single subsites. Thus, changes in the value of $K^p_{g3/4}$ as a function of active site substitution reflect changes in binding not only to subsites M3 and M4 but, for some variants, also to subsite M2 as well.

Because variant effects on the values of K^p_{g2} and $K^p_{g3/4}$ are unreliable as measures of effects on subsites M2, M3, and M4, we instead define a parameter R^p_{ov}, equal to the ratio $[K^p_{g2}(K^p_{g3/4})^2(\text{variant})/K^p_{g2}(K^p_{g3/4})^2(\text{wild-type})]$, to compare variant effects on overall Mg^{2+} binding to these subsites. The nonconservative active site variant D97V has the largest R^p_{ov}, 43. For the conservative variants, large (12−20) values are observed for E20D, K29R, D65E, D70E, and K142R, more moderate values (5−9) for E31D, R43K, and Y55F, and small R^p_{ov} values (1−3) for D67E, D97E, D102E, K104R, and Y141F.

The utility of comparing R^p_{ov} values is subject to limitations imposed by the equilibrium dialysis measurement technique and the multiple Mg^{2+} sites per subunit. Equilibrium dialysis measures Mg^{2+} bound as the difference between total Mg^{2+} concentration (the sum of free and bound Mg^{2+}) and free Mg^{2+} concentration. This restricts the useful range of free Mg^{2+} concentration to 5−10-fold the E-PPase concentration (the highest level employed was 1.0 mM, 20 mg/mL), since beyond this value the error in the difference does not permit accurate values to be obtained. This problem is exacerbated in the present case by the presence of multiple sites: i.e., estimation of a dissociation constant for a single weak site involves determining values of bound Mg^{2+}/PPase monomer of between 0.0 and 1.0, whereas estimation of a dissociation constant to a weaker site in the presence of tighter sites requires estimation of such values, for example, between 1.5 and 2.5, or between 2.5 and 3.5, which are inherently less accurate. Restriction of the useful range of free Mg^{2+} concentration has as a consequence that sites with dissociation constant values of >3 mM will only be partially occupied, making it difficult to distinguish average effects at each of the subsites M2−M4 from small effects at some and large effects on others. A case in point is the R43K variant. Recent X-ray diffraction results on crystals of the corresponding R78K variant of Y-PPase grown in the presence of Mn^{2+} and P_i show that while the M1, M2, M4, and P2 sites are filled, the M3 and P1 sites are unoccupied (*34*). In this case, a moderate R^p_{ov} value masks a dramatic effect on the M3 subsite.

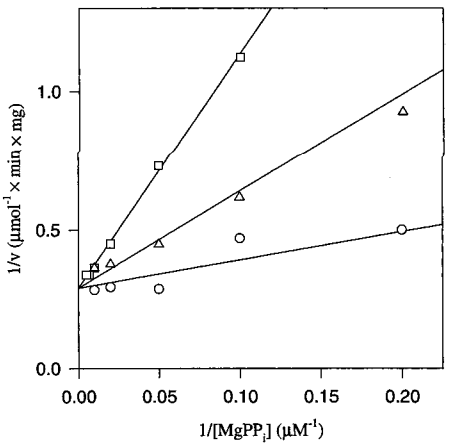

FIGURE 4: HMBP inhibition of the initial rate of WT-E-PPase-catalyzed PP_i hydrolysis at 20 mM Mg^{2+}. Lines drawn are to eq 4, at [HMBP] concentrations (μM) of 0 (○), 80 (△), and 240 (□) with K_m equal to 3.5 μM (*30*), and K_i equal to 33 μM.

Mg^{2+} Binding in the Presence of HMBP. HMBP, previously shown to be a competitive inhibitor of yeast (*35*) and mammalian PPases (*36*, *37*), is also a competitive inhibitor of E-PPase, with a K_i vs PP_i of 33 μM, measured at pH 7.2 and 20 mM Mg^{2+} (Figure 4). As seen in Figure 5, added HMBP (100 μM) parallels the effect of 20 mM P_i in inducing binding of additional Mg^{2+} per E-PPase subunit, presumably as the complex Mg_2HMBP, by analogy to the binding of Mg_2PP_i in Scheme 1. Proceeding as above, binding results for WT-E-PPase and E-PPase variants were fit to eq 2, yielding the values for K^{pp}_{g1}, K^{pp}_{g2}, and $K^{pp}_{g3/4}$ presented in Table 3. Also given in Table 3 are values for R^{pp}_{ov}, equal to the ratio $[K^{pp}_{g2}(K^{pp}_{g3/4})^2(\text{variant})/K^{pp}_{g2}(K^{pp}_{g3/4})^2(\text{wild-type})]$.

These values show some interesting similarities and differences vis-à-vis the corresponding constants determined in the presence of P_i. First, for WT-PPase, the values of these constants are more tightly bunched than the corresponding values measured in the presence of P_i [$K^{pp}_{g3/4}/K^{pp}_{g1}$ (equal to 19) < $K^p_{g3/4}/K^p_{g1}$ (equal to 62)], resulting from a 2-fold weakening of affinity for the first bound Mg^{2+} and a strengthening of third and fourth Mg^{2+} binding. Second, D65E substitution results in a large increase (5-fold) in K^{pp}_{g1}, paralleling the 5−7-fold effects seen on K^p_{g1} and K_{g1}, but the smaller (3-fold) effect that D102E substitution has on these latter constants is not seen on K^{pp}_{g1}. Third, although there is some correlation between R^{pp}_{ov} and R^p_{ov} values, there are some notable differences: (a) E31D and D65E have much smaller R^{pp}_{ov} values (0.5, 0.8) than R^p_{ov} values (9, 14);

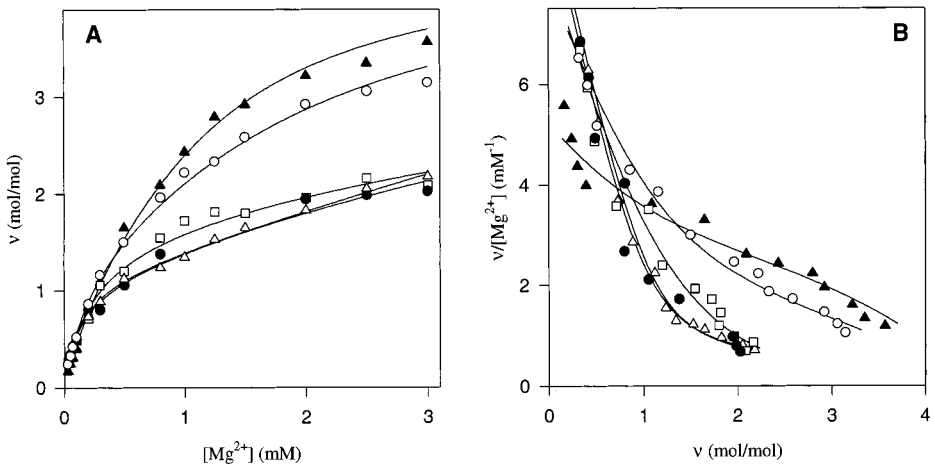

FIGURE 5: Mg^{2+} binding to WT-E-PPase and several E-PPase variants in the presence of 100 μM HMBP. Lines are fit to eq 2, using parameter values found in Table 3. Wild-type (○), E20D (□), D67E (▲), K104R (●), and K142R (△). (A) Binding curves. (B) Scatchard plots. Data are shown for three variants having weaker Mg^{2+} binding than wild-type, i.e., increased R^{pp}_{ov}, and one variant with stronger Mg^{2+} binding than wild-type (see Table 3).

Table 3: Mg^{2+} Binding in the Presence of 100 mM HMBP[a]

E-PPase	K^{pp}_{g1} (mM)	K^{pp}_{g2} (mM)	$K^{pp}_{g3/4}$ (mM)	R^{pp}_{ov}
WT	0.128 ± 0.004	0.73 ± 0.07	2.4 ± 0 0.2	1.0 ± 0.15
E20D	0.121 ± 0.007	0.90 ± 0.15	10 ± 2	21 ± 7
K29R	0.119 ± 0.003	1.6 ± 0.2	3.0 ± 0.3	3.5 ± 0.7
E31D	0.084 ± 0.005	1.2 ± 0.2	1.7 ± 0.2	0.8 ± 0.2
R43K	0.108 ± 0.006	3.6 ± 1.0	4.5 ± 1.3	17 ± 8
Y55F	0.088 ± 0.003	2.8 ± 0.5	4.4 ± 0.7	13 ± 4
D65E[b]	0.65 ± 0.06	0.65 ± 0.06	1.8 ± 0.5	0.5 ± 0.2
D67E	0.204 ± 0.009	0.75 ± 0.11	1.44 ± 0.14	0.4 ± 0.1
D70E	0.109 ± 0.005	2.7 ± 0.6	5.1 ± 1.3	17 ± 7
D97E	0.073 ± 0.005	0.83 ± 0.19	1.9 ± 0.3	0.7 ± 0.2
D102E[b]	0.173 ± 0.003	0.173 ± 0.003	1.8 ± 0.1	0.14 ± 0.01
K104R	0.106 ± 0.006	2.5 ± 0.8	8 ± 3	38 ± 24
Y141F[c]	0.097 ± 0.004	2.9 ± 0.1	2.9 ± 0.1	5.8 ± 0.4
K142R[c]	0.107 ± 0.004	5.2 ± 0.3	5.2 ± 0.3	33 ± 3
D97V	0.223 ± 0.009	4.5 ± 1.3	>20	>400

[a] Enzyme concentration 0.8−1.0 mM. [b] K^{pp}_{g1} set equal to K^{pp}_{g2} because the initial fitted values were indistinguishable from one another. [c] K^{pp}_{g2} set equal to $K^{pp}_{g3/4}$ because the initial fitted values were indistinguishable from one another.

(b) inversely, K104R and Y141F have much larger R^{pp}_{ov} values (38 and 6, respectively) than R^{p}_{ov} values (3 and 1, respectively); and (c) D102E actually enhances average Mg^{2+} binding to sites M2−M4 (R^{pp}_{ov} equal to 0.14), but has little effect on R^{p}_{ov}.

P_i Binding. In earlier studies on Y-PPase, we showed there to be a high-affinity P_i site ($K_d \sim 0.2$ mM) and a lower affinity site ($K_d \sim 1.6$ mM) in the presence of Mn^{2+} (*38*). As shown in Figure 6, in the presence of 100 μM Mn^{2+}, P_i also binds to a high-affinity site on E-PPase, with a dissociation constant (K_p) of 0.16 mM and a stoichiometry of 1.0/subunit. Binding to this site was also examined for the 13 conservative active site variants examined by our previous assays, and for 2 additional variants, K34R and E98V, as well. Most of these variants display decreased binding affinity (Table 4). The most potent effects (>50-fold increase in K_p) are seen for D70E and Y55F substitution. A second group of substitutions, showing increases in K_p from 8- to 36-fold, include E20D, K29R, E31D, R43K, D65E, and K142R. The remaining substitutions have only minor effects (relative K_p values of 0.5−3.3) except for D97E, which *decreases* K_p 9-fold.

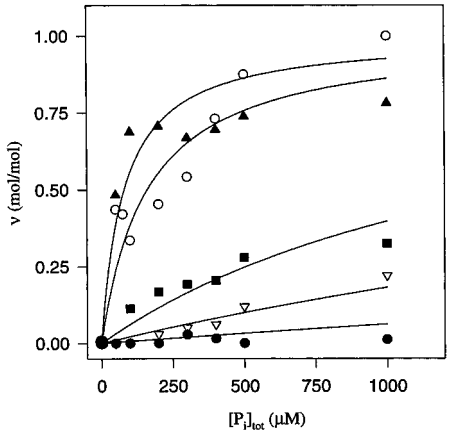

FIGURE 6: P_i binding to WT-E-PPase and several E-PPase variants in the presence of 100 μM Mn^{2+}. Lines are fit to eq 3, using parameter values found in Table 4. Wild-type (○), K29R (▽), R43K (■), D70E (●), and D97E (▲). Data are shown for variants having the full range of effects on P_i binding, from enhanced vs wild-type to strongly diminished (see Table 4).

Table 4: P_i Binding in the Presence of 100 mM Mn^{2+} [a]

E-PPase	K_p (mM)	relative K_p
WT	0.16 ± 0.02	1.00
E20D	1.3 ± 0.2	8.1
K29R	5.0 ± 0.6	31
E31D	5.8 ± 1.3	36
R43K	1.4 ± 0.1	8.8
Y55F	8.7 ± 2.1	54
D65E	3.0 ± 0.4	19
D67E	0.08 ± 0.01	0.5
D70E	>15	>90
D97E	0.018 ± 0.004	0.11
D102E	0.44 ± 0.03	2.8
K104R	0.40 ± 0.05	2.5
Y141F	0.52 ± 0.04	3.3
K142R	2.4 ± 0.4	15
K34R	0.21 ± 0.04	1.3
E98V	0.51 ± 0.03	3.2

[a] Enzyme concentration 0.5 mM.

DISCUSSION

The experiments reported in this paper are part of a broad effort to fully characterize the structure and function of

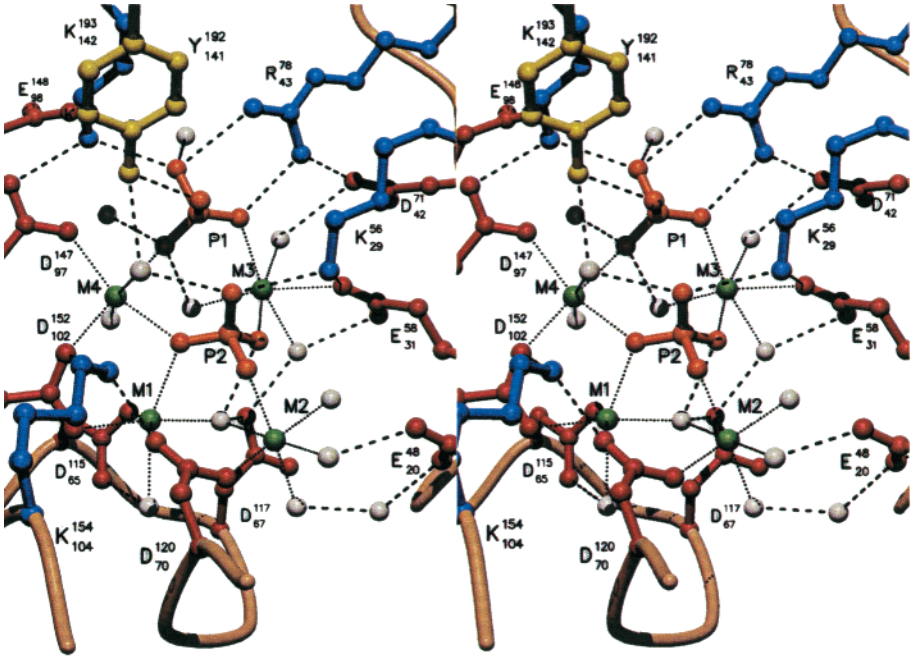

FIGURE 7: Stereo drawing of the active site of the Y-PPase $Mn_2E(MnP_i)_2$ complex. Acidic residues are in red and basic in blue; tyrosine is in yellow. Mn^{2+} ions (M1−M4) are shown in green; phosphates (P1, P2) in orange; and waters in gray. Both E-PPase (lower numbers) and Y-PPase (upper numbers) numbering is shown for the active site residues. Adapted from ref *21*.

type I soluble PPases. Here we demonstrate that the sensitivity to conservative substitution of active site residues of ligand binding to E-PPase varies considerably from residue to residue. The present results, considered in light of pertinent results from crystallographic studies on both E-PPase and Y-PPase and functional studies on Y-PPase, allow conclusions regarding (a) substitutions that induce general perturbation of active site structure; (b) specific subsite properties such as functional interaction with other subsites and flexibility; and (c) differences in the structure of enzyme-bound substrate (PP_i) and product ($2P_i$) complexes.

Interactions at the active site defined by X-ray crystallography (Figure 7) are summarized in Table 5, which includes results for the $Mg_{1.5}E$ (*23*), $Mg_{2.5}E$ (*24*), and sulfate (*25*) complexes of E-PPase, and the Mn_2E, $Mn_2E(MnP_i)_2$ (product), and $Mn_2EMn_2FPP_i$ complexes of Y-PPase (*21*, *22*, *26*). These interactions provide an excellent framework for interpreting the effects of active site substitution determined in this work. That the interpretation of the E-PPase results presented in this paper is based in part on Y-PPase structures is reasonable based on the high degree of structural and functional similarity between these two enzymes (*15*, *20*, *21*, *39*, *40*). In what follows we use E-PPase numbering for both E-PPase residues and the aligned, conserved active site residues in Y-PPase (*15*, *20*).

Subsites M1 and M2 in E-PPase. Our results for these subsites are reasonably straightforward to interpret because K_{g1}, K_{n1}, K^{p}_{g1}, and K^{pp}_{g1} provide direct measures of metal ion dissociation from M1, and K_{g2}, K_{n2}, and, for the most part, K^{p}_{g2} provide direct measures of metal ion dissociation from M2.

Particularly striking for M1 is the similarity of the K_{g1}, K^{p}_{g1}, and K^{pp}_{g1} values, not only for WT-E-PPase but also for each of the conservative active site variants (Tables 1−3). This suggests that site M1 is functionally rather isolated from the remainder of the active site, in the sense that P_i or HMBP binding has little effect on M1 binding. Evidence that P_i binds to site P1 in the absence of divalent metal ion comes from the crystal structure of the sulfate complex of E-PPase (*25*) and from P_i inhibition of R43 modification (*38*). The estimated dissociation constant for P_i binding to form EP_i is ~1 mM (*38*). Thus, K^{p}_{g1}, determined in the presence of 20 mM P_i, measures Mg^{2+} binding to a mixture of E and EP_i, in which EP_i predominates. In a parallel fashion, the similarity of K_{g1} and K^{pp}_{g1} values shows that Mg^{2+} affinity is little affected by HMBP at the active site, making the reasonable assumption that this ligand also binds to the active site in the absence of divalent metal ion.

Site M1 interacts directly with D65, D70, and D102, and via water with D67 (Table 5, Figure 7), yet conservative

Table 5: Correlation of Ligand Contacts[a] and Substitution Effects in PPase

residue or P_i site[b]	M1	M2	M3	M4	P1	P2	substitution effects[c]
E20(D)	−	vw	−	−	−	−	L/L/M
K29(R)	−	−	−	−	(d)[d]	d	L/M/L
E31(D)	−	−	d	−	−	−	M/S/L
R43(K)	−	−	−	−	d	−	M/L/M
Y55(F)	−	−	−	−	−	d	L/M/VL
D65(E)	d	−	−	vw	−	−	L/S/L
D67(E)	vw	vw	vw	−	−	vw	S/S/S
D70(E)	d	d	−	−	−	−	L/L/VL
D97(E)	−	−	−	d	−	−	S/S/dec
D102(E)	d	−	−	d	−	−	S/dec/S
K104(R)	−	−	−	vw	−	vw	S/L/S
Y141(F)	−	−	−	vw	d	vw	S/M/S
K142(R)	−	−	−	−	d	−	L/L/L
P1	−	−	d	d			
P2	d	d	d	d			

[a] As reported in refs *21*, *23*−*25*. Abbreviations: d, direct; vw, via water; −, no contact. [b] Parentheses show substitutions, the effects of which are presented in the last column. [c] Effects of substitution on R^{p}_{ov}/R^{pp}_{ov}/relative K_p: VL, >50-fold; L, >10−40-fold; M, 3.5−9-fold; S, 0.4−3-fold; dec, decrease. [d] Seen only in the sulfate complex of E-PPase (*25*).

D/E substitution at only D65 results in a large increase in K_{g1}, K_{n1}, K^{p}_{g1}, and K^{pp}_{g1} values (5−15-fold). The corresponding range for D102E substitution is 1−3-fold, and no other conservative substitution, including D67E and D70E, leads to a >2-fold increase in any of these four constants. In addition, the nonconservative D102V substitution increases K_{g1} 11-fold, placing an upper limit on the contribution of the negative charge on D102 to M1 binding, as contrasted with <2-fold increases on D97V or E98V substitution.

D65E substitution significantly reduces ligand affinity, not only to site M1, but also to other sites, as measured by R^{p}_{ov}, $K_{g:in}$, and K_p, so that it appears that the structural perturbation resulting from this substitution is propagated elsewhere in the active site as well as to the trimer−trimer interface. On the other hand, D67E and D102E substitutions apparently do not cause long-range perturbations of the active site, since they neither cause major reduction in M1 affinity nor significantly reduce any other measures of ligand affinity reported here (Tables 1−4).

In contrast, D70E substitution, while little affecting binding to M1 or M2, clearly results in major perturbation of the active site. D70E-PPase has by far the lowest enzymatic activity of all of the conservative active site variants we have characterized (*16*, *20*). In addition, despite the lack of direct interaction of D70 with P1, P2, M3, or M4, D70E substitution dramatically decreases not only P_i binding (Table 4) but also both P_i- and HMBP-induced Mg^{2+} binding (Tables 2 and 3). Furthermore, the structure of the related D70N variant of E-PPase shows large-scale reorganization of the active site, despite relatively little motion at N70 with respect to WT-E-PPase (*41*). It would thus appear that the D70 side chain occupies a critical location for maintaining the overall structure of the active site. We believe it likely that while local flexibility allows the carboxylate side chain in the D70E variant to fully participate in M^{2+} binding to both M1 and M2, the resulting need to accommodate the extra methylene of the variant induces a distortion that is propagated throughout the active site.

Site M2 interacts directly with D70 and via water with E20 and D67, but of all the conservative variants studied, only E20D substitution substantially increases either K_{g2} or K^{p}_{g2}. In addition, E20D substitution promotes dissociation of E-PPase hexamer into trimers (*18*) and leads to large increases in $K_{g:in}$, R^{p}_{ov}, R^{pp}_{ov}, and K_p, despite the lack of any direct contact of E20 either with subsites other than M2 (Table 5) or with the trimer−trimer interface. Accordingly, it appears not only that E20D substitution distorts the M2 subsite but also that this distortion is propagated throughout the enzyme structure, at the active site and reaching to the trimer−trimer interface.

Subsites M1 and M2: E-PPase vs Y-PPase. Despite the extensive structural and functional similary between the active sites of E-PPase and Y-PPase (*20*, *21*, *40*), some interesting differences are also apparent. For example, WT-Y-PPase binds metal ions to sites M1 and M2 37- and 190-fold more tightly than WT-E-PPase, respectively (*12*). In addition, the effects of mutation of aligned residues in Y-PPase and E-PPase differ both qualitatively and quantitatively. In contrast to what is seen for E-PPase variants (Table 1), every Y-PPase variant examined showed a significant effect on metal ion binding to M2 (*42*). Further, the sensitivity of M1 binding to two D/E mutations is inverted. Thus, for E-PPase, D65E substitution significantly decreases affinity and D70E substitution has little effect (Table 1), whereas for Y-PPase D115E substitution has no effect on M1 binding but D120E substitution has a significant effect (*42*). These differences in metal ion binding properties are most probably due to the closer packing of the Y-PPase active site.

Subsites M3, M4, P1, and P2. Addition of either P_i or HMBP induces binding to M3 and M4. Many active site substitutions affect both P_i- and HMBP-induced Mg^{2+} binding (Tables 2 and 3) as well as P_i binding (Table 4). This is not unexpected, since in all three cases such effects can arise from perturbations at metal-ion and/or phosphoryl group binding subsites. Interpretation of effects on K_p is further complicated by two additional factors. First, the apparent effects on K_p may only represent lower limits, since severe distortion of the high-affinity site may result in binding of the first P_i to the lower affinity site. Second, there is some ambiguity concerning the identity of the high-affinity P_i site. Zyranov et al. (*43*) have recently demonstrated for Y-PPase that this identity is divalent metal ion dependent, with P2 being the high-affinity site in the presence of Mn^{2+}, whereas P1 is the high-affinity site either in the presence of Mg^{2+} (*8*, *44*) or in the absence of divalent metal ion altogether (see above). Our results for substitution effects on K_p would tend to support this ordering for E-PPase in the presence of Mn^{2+} as well. Thus, Y55 binds directly to P2 rather than to P1 (Table 5), and, apart from D70E substitution, which results in a general perturbation of the active site, Y55F substitution causes the largest increase in K_p (Table 4). By contrast, Y141 binds directly to P1 and not to P2, and Y141F substitution has only a modest effect on K_p. Moreover, substitutions of aligned residues in E-PPase and Y-PPase have similar weakening effects on high-affinity P_i binding. Thus, for Y-PPase, the effects fall in the order (in E-PPase numbering) Y55F > K29R > R43K, K142R (*43*), paralleling what is reported in Table 4.

As a result of these factors, substitution effects cannot, in general, be attributed to single subsites, as is possible for M1 and, for most variants, for M2. Rather, it is more appropriate to consider the parameters R^{p}_{ov}, R^{pp}_{ov}, and K_p as providing different measures of overall ligand affinity to subsites M3, M4, P1, and P2, and, for some variants, to M2. The effects of conservative substitution on these parameters, as summarized in Table 5, reflect alterations at one or more of these subsites, arising from direct perturbation of a binding interaction, or from a perturbation that is propagated within the active site cavity.

Despite these inherent ambiguities, the results in Table 5 permit three further conclusions: first, that K142, like E20, D65, and D70, plays a key role in the functional organization of the active site, since K142R substitution induces large increases in R^{p}_{ov}, R^{pp}_{ov}, and K_p as well as in K_m for Mg_2PP_i (*20*); second, that the M4 subsite is an especially unconstrained part of the active site. This conclusion derives from the observation that conservative substitutions of three of the four amino acid side chains interacting directly or via water with this subsite (D97, D102, and Y141) result in no large decreases in ligand affinity (the exception is D65E substitution, which causes a general perturbation). Supporting this conclusion, the D97−D102 loop, including the two residues binding directly to M4, is disordered in some

E-PPase structures (*45*) and undergoes the largest motions between the Mn_2-Y-PPase and Mn_2-Y-PPase$(MnPi)_2$ structures (*21*). The third conclusion is that the major differences between the product and substrate complexes of E-PPase are concentrated in the lower half of the active site (Figure 7). This conclusion, which is consistent with recent structural studies on Y-PPase (*22*), is based on the observation that the four substitutions showing the greatest differences in effects on R^{p}_{ov} vs R^{pp}_{ov}, E31D, D65E, D102E, and K104R, all fall within the lower half of the active site. Moreover, the polar termini of D65, D102, and K104 are quite close to one another (Figure 7 and ref *16*) and are centered about D102, within the flexible 97−102 loop.

ACKNOWLEDGMENT

We thank Vesa Tuominen for making Figure 7 and Alex Baykov and Pekka Pohjanjoki for helpful suggestions.

REFERENCES

1. Chen, J., Brevet, A., Formant, M., Leveque, F., Schmitter, J.-M., Blanquet, S., and Plateau, P. (1990) *J. Bacteriol. 172*, 5686−5689.
2. Lundin, M., Baltscheffsky, H., and Ronne, H. (1991) *J. Biol. Chem. 266*, 12168−12172.
3. Sonnewald, U. (1992) *Plant J. 2*, 571−581.
4. Kornberg, A. (1962) in *Horizons in Biochemistry* (Kasha, H., and Pullman, P., Eds.) pp 251−264, Academic Press, New York.
5. Sivula, T., Salminen, A., Parfenyev, A. N., Pohjanjoki, P., Goldman, A., Cooperman, B. S., Baykov, A. A., and Lahti, R. (1999) *FEBS Lett. 454*, 75−80.
6. Young, T. W., Kuhn, N. J., Wadeson, A., Ward., S., Burges, D., and Cooke, G. D. (1998) *Microbiology 144*, 2563−2571.
7. Shintani, T., Uchiumi, T., Yonezawa, T., Salminen, A., Baykov, A. A., Lahti, R., and Hachimori, A. (1998) *FEBS Lett. 439*, 263−266.
8. Springs, B., Welsh, K. M., and Cooperman, B. S. (1981) *Biochemistry 20*, 6384−6391.
9. Baykov, A. A., Shestakov, A. S., Kasho, V. N., Vener, A. V., and Ivanov, A. H. (1990) *Eur. J. Biochem. 194*, 879−887.
10. Baykov, A. A., Hyytiä, T., Volk, S. E., Kasho, V. N., Vener, A. V., Goldman, A., Lahti, R., and Cooperman, B. S. (1996) *Biochemistry 35*, 4655−4661.
11. Baykov, A. A., Fabrichniy, I. P., Pohjanjoki, P., Zyryanov, A. B., and Lahti, R. (2000) *Biochemistry 39*, 11939−11947.
12. Belogurov, G. A., Fabrichniy, I. P., Pohjanjoki, P., Kasho, V., Lehtihuhta, E., Turkina, M. V., Cooperman, B. S., Goldman, A., Baykov, A. A., and Lahti, R. (2000) *Biochemistry 39*, 13931−13938.
13. Lahti, R., Pitkäranta, T., Valve, E., Ilta, I., Kukko-Kalske, E., and Heinonen, J. (1988) *J. Bacteriol. 170*, 5901−5907.
14. Kolakowski, L., Schlösser, M., and Cooperman, B. S. (1988) *Nucleic Acids Res. 16*, 10441−10452.
15. Cooperman, B. S., Baykov, A. A., and Lahti, R. (1992) *Trends Biochem. Sci. 17*, 262−266.
16. Salminen, T., Käpylä, J., Heikinheimo, P., Kankare, J., Goldman, A., Heinonen, J., Baykov, A. A., Cooperman, B. S., and Lahti, R. (1995) *Biochemistry 34*, 782−791.
17. Heikinheimo, P., Pohjanjoki, P., Helminen, A., Tasanen, M., Cooperman, B. S., Goldman, A., Baykov, A. A., and Lahti, R. (1996) *Eur. J. Biochem. 239*, 138−143.
18. Volk, S. E., Dudarenkov, V. Yu., Käpylä, J., Kasho, V. N., Voloshina, O. A., Salminen, T., Goldman, A., Lahti, R., Baykov, A. A., and Cooperman, B. S. (1996) *Biochemistry 35*, 4662−4669.
19. Fabrichniy, I. P., Kasho, V. N., Hyytiä, T., Salminen, T., Halonen, P., Dudarenkov, V. Yu., Heikinheimo, P., Chernyak, V. Ya., Goldman, A., Lahti, R., Cooperman, B. S., and Baykov, A. A. (1997) *Biochemistry 36*, 7746−7753.
20. Pohjanjoki, P., Lahti, R., Goldman, A., and Cooperman, B. S. (1998) *Biochemistry 37*, 1754−1761.
21. Heikinheimo, P., Lehtonen, J., Baykov, A. A., Lahti, R., Cooperman, B. S., and Goldman, A. (1996) *Structure, 4*, 1491−1508.
22. Heikinheimo, P., Tuominen, V., Ahonen, A.-K., Teplyakov, A., Cooperman, B. S., Baykov, A. A., Lahti, R., and Goldman, A. (2001) *Proc. Natl. Acad. Sci. U.S.A.* (in press).
23. Kankare, J., Salminen, T., Lahti, R., Cooperman, B., Baykov, A. A., and Goldman, A. (1996) *Biochemistry 35*, 4670−4677.
24. Haruryunyan, E. H., Oganessyan, V. Yu., Oganessyan, N. N., Avaeva, S. M., Nazarova, T. I., Vorobyeva, N. N., Kurilova, S. A., Huber, R., and Mather, T. (1997) *Biochemistry 36*, 7754−7760.
25. Avaeva, S., Kruilova, S., Nazarova, T., Rodina, E., Vorobyeva, N., Sklyankina, V., Grigorjeva, O., Haurtyunyan, E., Oganessyan, V., Wilson, K., Dauter, Z., Huber, R., and Mahler, T. (1997) *FEBS Lett. 410*, 502−508.
26. Harutyunyan, E. H., Kuranova, I. P., Vainshtein, B. K., Hohne, W. E., Lamzin, V. S., Dauter, Z., Teplyakov, A. V., and Wilson, K. S. (1996) *Eur. J. Biochem. 239*, 220−238.
27. Efimova, I. S., Salminen, A., Pohjanjoki, P., Lapinniemi, J., Magretova, N. N., Cooperman, B. S., Goldman, A., Lahti, R., and Baykov, A. A. (1999) *J. Biol. Chem. 274*, 3294−3299.
28. Lahti, R., Pohjanoksa, K., Pitkäranta, T., Heikinheimo, P., Salminen, T., Meyer, P., and Heinonen, J. (1990) *Biochemistry 29*, 5761−5766.
29. Baykov, A. A., and Avaeva, S. M. (1981) *Anal. Biochem. 116*, 1−4.
30. Käpylä, J., Hyytiä, T., Lahti, R., Goldman, A., Baykov, A. A., and Cooperman, B. S. (1995) *Biochemistry 34*, 792−800.
31. Duggleby, R. (1984) *Comput. Biol. Med. 14*, 447−455.
32. Baykov, A. A., Dudarenkov, V. Yu., Käpylä, J., Salminen, T., Hyytiä, T., Kasho, V. N., Husgafvel, S., Cooperman, B. S., Goldman, A., and Lahti, R. (1995) *J. Biol. Chem. 270*, 30804−30812.
33. Baykov, A. A., Hyytiä, T., Turkina, M. V., Efimova, I. S., Kasho, V. N., Goldman, A., Cooperman, B. S., and Lahti, R. (1999) *Eur. J. Biochem. 260*, 308−317.
34. Tuominen, V., Heikinheimo, P., Kajander, T., Torkkel, T., Hyytiä, T., Käpylä, J., Lahti, R., Cooperman, B. S., and Goldman, A. (1998) *J. Mol. Biol. 284*, 1565−1580.
35. Cooperman, B. S., and Chiu, N. Y. (1973) *Biochemistry 12*, 1676−1682.
36. Smirnova, I. N., Kudryavtseva, N. A., Komissarenko, S. V., Tarusova, N. B., and Baykov, A. A. (1988) *Arch. Biochem. Biophys. 267*, 280−284.
37. Smirnova, I. N., and Baykov, A. A. (1991) *Arch. Biochem. Biophys. 287*, 135−140.
38. Cooperman, B. S., Panackal, A., Springs, B., and Hamm, D. (1981) *Biochemistry 20*, 6051−6060.
39. Kankare, J., Neal, G. S., Salminen, T., Glumoff, T., Cooperman, B., Lahti, R., and Goldman, A. (1994) *Protein Eng. 7*, 823−830.
40. Baykov, A. A., Cooperman, B. S., Goldman, A., and Lahti, R. (1999) *Prog. Mol. Subcell. Biol. 23*, 127−150.
41. Avaeva, S. M., Rodina, E. V., Vorobyeva, N. N., Kurilova, S. A., Nazarova, T. I., Sklyankina, V. A., Oganessyan, V. Y., Samygina, V. R., and Harutyunyan, E. H. (1998) *Biochemistry (Moscow) 63*, 671−684.
42. Pohjanjoki, P., Fabrichniy, I. P., Kasho, V. N., Cooperman, B. S., Goldman, A., Baykov, A. A., and Lahti, R. (2001) *J. Biol. Chem. 276*, 434−441.
43. Zyryanov, A. B., Pohjanjoki, P., Kasho, V. N., Shestakov, A. S., Goldman, A., Lahti, R., and Baykov, A. A. (2001) *J. Biol. Chem.*, in press.
44. Kasho, V. N., and Baykov, A. A. (1989) *Biochem. Biophys. Res. Commun. 161*, 6384−6391.
45. Kankare, J., Salminen, T., Lahti, R., Cooperman, B., Baykov, A. A., and Goldman, A. (1996) *Acta Crystallogr. D52*, 551−563.

BI010049X